

# NMR Relaxation Studies of the Role of Conformational Entropy in Protein Stability and Ligand Binding

MARTIN J. STONE\*

Department of Chemistry, Indiana University,  
800 East Kirkwood Avenue,  
Bloomington, Indiana 47405-0001

Received November 14, 2000

## ABSTRACT

Recent advances in the measurement and analysis of protein NMR relaxation data have made it possible to characterize the dynamical properties of many backbone and side chain groups. With certain caveats, changes in flexibility that occur upon ligand binding, mutation, or changes in sample conditions can be interpreted in terms of contributions to conformational entropy. Backbone and side chain flexibility can either decrease or increase upon ligand binding. Decreases are often associated with “enthalpy–entropy compensation” and “induced fit” binding, whereas increases in conformational entropy can contribute to stabilization of complexes. In certain cases, conformational entropy appears to play a role in cooperative binding and enzyme catalysis. In addition, variations in conformational entropy and heat capacity may both be important in stabilizing the folded structures of proteins.

## Introduction

A thorough understanding of biomolecular recognition events requires evaluation of the various physical effects contributing to binding free energy. Although net enthalpy and entropy changes can be determined by conventional thermodynamic methods, each of these is generally the sum of several much larger, but often opposing, contributions, making the assessment of individual terms difficult. Indirect estimates of individual contributions are commonly deduced from the effects of mutations or changes in ligand structure (i.e., structure–activity relationships). However, in practice it is generally difficult to make modifications that influence any one factor selectively. Thus, alternative approaches that allow more direct observation of individual physical effects would be extremely advantageous in advancing our understanding of many systems.

Recent advances in the measurement and analysis of protein NMR relaxation data have made it possible to characterize the dynamical properties of many backbone and side chain groups.<sup>1–4</sup> Subject to certain assumptions (vide infra), these motions can be related to conforma-

tional entropy. Thus, differences in this entropy term upon changes in the state of the protein (binding, folding, etc.) can be estimated from these data. In this Account, I briefly describe the methods that are used to obtain such estimates of conformational entropy and then review the recent literature in which NMR data have indicated the importance of conformational entropy (and heat capacity) in ligand binding and protein folding.

The potential importance of conformational entropy in contributing to the stability of folded proteins and their complexes is illustrated by the popular “protein folding funnel”, the width of which is a representation of conformational entropy<sup>5</sup> (Figure 1). As the protein folds, the width of the funnel narrows, corresponding to a dramatic restriction of backbone and side chain motions. For even a small protein, this loss of conformational entropy is estimated to cost as much as several hundred kilojoules per mole at 25 °C.<sup>6</sup> However, the bottom of the folding funnel retains some finite width and roughness, indicating that even a folded protein is not restricted to a single conformational state but rather undergoes fluctuations between a number of states separated by small energy barriers. Even a subtle change in the landscape at the bottom of the funnel could therefore make substantial changes to conformational entropy, which could contribute to the relative stability of proteins and their complexes.

## Estimation of Conformational Entropy from NMR Relaxation Data

The flow of information from measured NMR relaxation parameters to calculated conformational entropy and heat capacity is represented schematically in Figure 2. The magnetic relaxation of nuclei is stimulated by magnetic fields oscillating at the relevant transition frequencies. The two predominant relaxation mechanisms (dipolar and chemical shift anisotropy<sup>7</sup>) both result from oscillations of the protein structure. Thus, protein motion (at the appropriate frequencies) can be detected on the basis of its influence on relaxation parameters. For example, the relaxation of a protonated <sup>15</sup>N nucleus (e.g., backbone amide) is influenced by NH group motions at the resonant frequencies of the nitrogen ( $\omega_N$ ) and the proton ( $\omega_H$ ), the sum and difference of these frequencies, and a frequency of zero (corresponding to loss of phase coherence without net energy loss) (Figure 3A). If enough independent relaxation parameters are measured, it is possible to calculate the density of motions [spectral density,  $J(\omega)$ ] at each of these five frequencies.<sup>8</sup> With modern spectrometers, most of these frequencies are in the 50–880 MHz range. Thus, this direct approach provides a rather limited sampling of the wide range of motional time scales that may occur in a typical protein.

Measurement of five or more different relaxation parameters has until recently been difficult (and remains tedious). Consequently, there has been considerable interest in obtaining useful dynamical information from fewer

Martin J. Stone received his B.Sc. and M.Sc. (honors) degrees from the University of Auckland, New Zealand (1986 and 1987, respectively), and his Ph.D. from Cambridge University, England (1991), under the tutelage of Dr. Dudley Williams. After completing a postdoctoral fellowship at the Scripps Research Institute, La Jolla, CA, with Dr. Peter Wright, he joined the faculty of the Chemistry Department at Indiana University, where he is currently Assistant Professor. His research focuses on the relationships of protein dynamics to structure, stability, and ligand binding, and on structure–activity relationships of chemokines.

\*Phone: 812-855-6779. Fax: 812-855-8300. E-mail: mastone@indiana.edu.

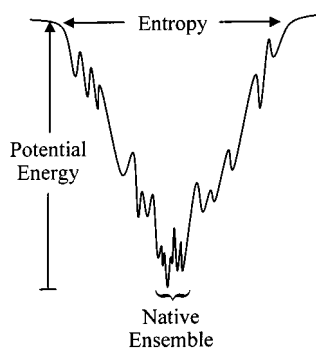


**FIGURE 1.** A protein folding funnel, illustrating that the native structure of a protein often retains considerable residual conformational entropy.

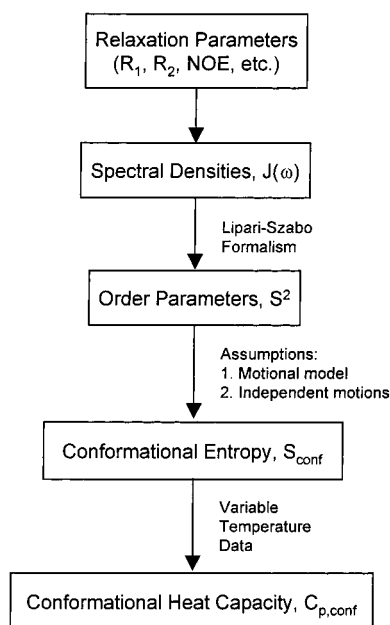


**FIGURE 2.** Flowchart illustrating the typical steps for interpretation of measured NMR relaxation parameters in terms of conformational entropy and heat capacity. See the text for a discussion of the limitations of this approach.

measured parameters. Most of these efforts have utilized the Lipari–Szabo “model-free” formalism<sup>9,10</sup> (Figure 3B), in which the spectral density function is defined in terms of (1) the global rotational diffusion of the macromolecule (molecular correlation time,  $\tau_m$ , typically a few nanoseconds, and possibly the diffusion anisotropy); (2) the time scale of internal motions faster than the global tumbling (effective internal correlation time,  $\tau_e$ , picosecond to nanosecond time scale); and (3) the degree of restriction (related to amplitude) of these fast internal motions (the square of the order parameter,  $S^2$ ). Extensions of this formalism have been developed to incorporate two time scales of internal motion or to account for the effects of slow (microsecond to millisecond time scale) conformational exchange.<sup>11–13</sup> Typically, three relaxation parameters [longitudinal ( $R_1$ ) and transverse ( $R_2$ ) relaxation rates and heteronuclear nuclear Overhauser enhancement ( $\{^1\text{H}\}$ – $^{15}\text{N}$  NOE)] are measured for each nucleus, and nonlinear fitting methods are used to find a single global rotational diffusion tensor and a set of internal dynamics parameters

for each nucleus. This approach has become popular because it is conceptually simple and relatively convenient to implement. However, the dynamics parameters obtained by this method are considered to be “model-free” in that they do not allow one to identify the exact nature of the motion experienced by each group. Nevertheless, interpretation of the model-free parameters within the framework of a given motional model (e.g., the diffusion-in-a-cone model, Figure 3C,D) often yields a physically reasonable picture;<sup>12</sup> e.g., a typical backbone NH group order parameter of 0.8 corresponds to a cone semiangle of 22°.

Order parameters ( $S^2$ ) are related to conformational entropy ( $S_{\text{conf}}$ ) because they indicate the range of structural states accessible to a bond vector. Three groups have put forward quantitative approaches to estimating conformational entropy from order parameters.<sup>14–17</sup> The most commonly used approach, which assumes that bond vector motions are approximated by the diffusion-in-a-cone model, yields the following relationship between  $S_{\text{conf}}$  and  $S$  (the Lipari–Szabo order parameter) for an isolated bond vector:<sup>16</sup>

$$S_{\text{conf}} = k_B \ln[\pi(3 - \sqrt{1 + 8S})] \quad (1)$$

in which  $k_B$  is Boltzmann’s constant. Using this or similar relationships, and order parameters for two states of a protein, it is possible to estimate the change in conformational entropy ( $\Delta S_{\text{conf}}$ ) between the two states.

Despite the initial attractiveness of this approach, it has the following significant shortcomings that complicate interpretation of the calculated entropy values. First, entropy estimates require assumptions to be made regarding the physical nature of the bond vector motion (or the mathematical form of the partition function), so the values obtained depend on the model chosen. This limitation may not be severe since  $\Delta S_{\text{conf}}$  values calculated using various reasonable motional models are consistent within roughly a factor of 2.<sup>16</sup>

A more significant problem is that the total entropy change calculated by using the above approach for multiple bond vectors is valid only if the motions of the individual bond vectors are truly independent. However, there is now substantial evidence for the existence of correlated motions. Variation of order parameters between different bond vectors within an amino acid can be understood by invoking correlated movement (e.g., “crankshaft” motion) of the backbone and side chain groups.<sup>18–20</sup> In addition, correlations between backbone order parameters and side chain volumes suggest that the motion of backbone NH groups is often coupled to the motion of the side chain in the same amino acid as well as neighboring residues.<sup>21</sup> In contrast, there is at least one case in which changes in side chain order parameters have been observed without corresponding changes in backbone parameters, suggesting a low level of motional correlation.<sup>22</sup> Although it is difficult to estimate the extent of correlated motions, complete independence of motions seems highly unlikely. From this perspective, entropy

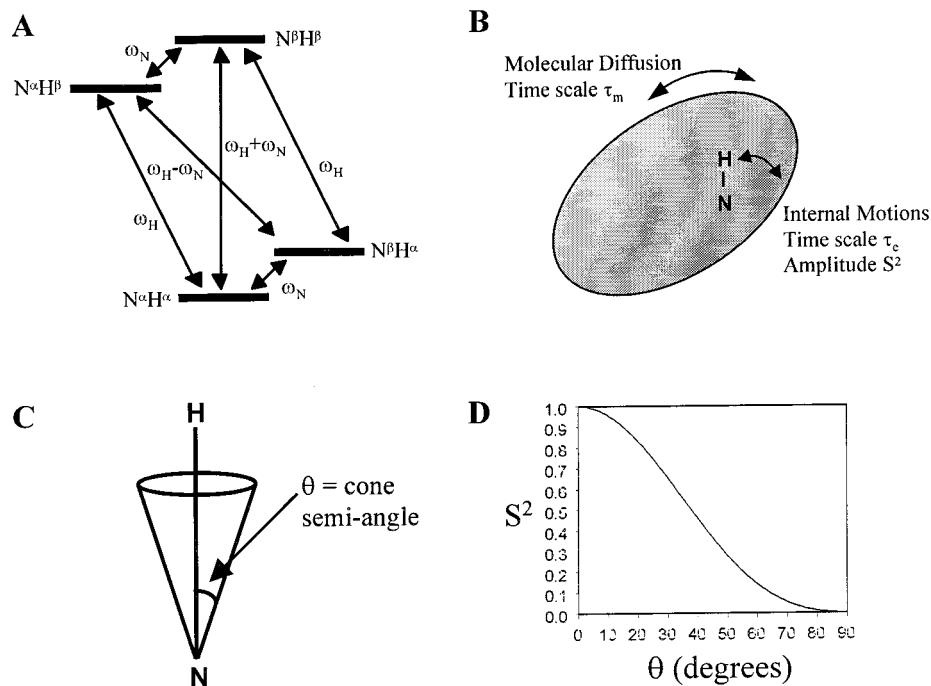


**FIGURE 3.** Relaxation and dynamics of an isolated NH group. (A) Energy level diagram for a  $^{15}\text{N}$ – $^1\text{H}$  spin pair, showing the frequencies of transitions that contribute to observable relaxation parameters. (B) Representation of the Lipari–Szabo model-free formalism, in which bond vector motions are mathematically separated into the global tumbling of the protein and internal rotational oscillations of the NH bond vectors relative to the molecular frame. (C) The diffusion-in-a-cone model of NH group motion; the NH bond vector is allowed to diffuse freely within the cone but not to sample the space outside of the cone. (D) Relationship between the square of the Lipari–Szabo order parameter ( $S^2$ ) and the cone semi-angle ( $\theta$ ) as defined in (C); this curve is described by the equation  $S^2 = [0.5 \cos \theta (1 + \cos \theta)]^2$ .

changes calculated from order parameters should be considered an upper limit (in magnitude).

A further difficulty with deriving conformational entropy values from order parameters is that NMR relaxation experiments are sensitive to only a subset of motions expected to be present in a protein. Typically, dynamics parameters are derived only for a limited group of bond vectors in the protein, so the contributions to entropy from undetected bond vectors remain unknown. This is being addressed by the development of novel experiments to probe the motions of an increasing number of bond vectors.<sup>2</sup> However, even for the bond vectors that are detected, order parameters are indicative only of rotational motions (those in which the bond vector is reoriented relative to the permanent magnetic field), whereas translational motion (e.g., bond stretching) remains undetected. Furthermore, order parameters are insensitive to motions on time scales slower than the molecular correlation time. Although NMR-based methods exist to probe structural fluctuations on slower time scales (e.g., exchange broadening measurements, saturation transfer, line shape analysis, and hydrogen–deuterium exchange), these methods do not generally reveal the amplitude of the motion, so relating them to entropy is difficult. If the conformational entropy components associated with undetected motions undergo changes similar to those undergone by the detected components, then one might surmise that the total entropy change calculated by the above method is, in fact, an underestimate. However, it is also possible that undetected components remain unchanged or change in the opposite direction to the

detected motions. A particular concern is that, in certain cases, the quenching of fast time scale motions may be accompanied by an increase in slower time scale motions, reflecting an increase in the activation energy barrier (for bond vector motion) without any change in the number of accessible conformational states (entropy).

Taken together, these issues introduce considerable uncertainty into values of conformational entropy estimated from order parameters. Nevertheless, if one limits discussion to the components of motion that are detected in the NMR experiments (fast time scale, rotational motions of the relevant bond vectors), it is probably reasonable to present entropy values calculated by the above method and to consider them as upper limits of the relevant entropy component (due to the possibility of correlated motions). The discussion presented below focuses on changes in picosecond to nanosecond time scale motion. The likely influences of these motions on ligand affinity and protein stability have been deduced either from the calculated entropy values or directly from order parameters. It is important to keep the above limitations in mind throughout this discussion.

## Backbone Entropy and Ligand Binding

Qualitative or quantitative measures of changes in conformational entropy upon ligand binding can be obtained by comparing order parameters, spectral densities, or relaxation parameters for a protein in the presence and in the absence of a ligand. Backbone dynamics have generally been determined by analysis of backbone  $^{15}\text{N}$

**Table 1. Changes in Protein Backbone Dynamics Observed upon Ligand Binding**

protein	ligand	observed changes	refs
Metal Ion Binding			
calbindin-D <sub>9k</sub>	Ca <sup>2+</sup> or Cd <sup>2+</sup>	binding to either site slightly reduces mobility of site I and greatly reduces mobility of site II	23, 24
cardiac troponin C	Ca <sup>2+</sup>	binding to site II reduces flexibility of both sites	25
skeletal troponin C	Ca <sup>2+</sup> <sup>a</sup>	larger reduction in entropy for site I than site II	26
Small Molecule Binding			
FKBP-12	FK506	reduced flexibility of loop at binding site	27
acyl-coenzyme A binding protein	palmitoyl-coA	reduced mobility of residues near binding site	28
intestinal fatty acid binding protein	palmitate	reduced motion of proposed ligand entry "portal"	29, 30
CcrA metallo- $\beta$ -lactamase	SB225666 (inhibitor)	reduced flexibility of active site loop (backbone and side chain)	31
ribonuclease T1	2'-GMP (competitive inhibitor)	decreased motion of active site loop; increased motion of loop distant from active site	32
stromelysin (matrix metallo-protease)	3 inhibitors <sup>b</sup>	binding to S <sub>1</sub> '-S <sub>3</sub> ' subsite reduces its flexibility but increases mobility of some surface residues; binding to S <sub>1</sub> -S <sub>2</sub> subsite does not influence its flexibility (already rigid)	33
4-oxalocrotonate tautomerase	<i>cis</i> , <i>cis</i> -muconate	compensating increases and decreases in entropy	34
major urinary protein (MUP-I)	2- <i>sec</i> -butyl-4,5-dihydro-thiazole	increased motions throughout protein	35
Peptide Binding			
insulin receptor substrate 1 pTyr-binding domain	phosphotyrosine-containing peptide	reduced mobility of residues that contact peptide	36
PLC- $\gamma$ 1 C-terminal SH2 domain	phosphotyrosine-containing peptide	one residue interacting with pTyr is rigidified; residues interacting with hydrophobic region become more flexible	37
calmodulin	peptide from myosin light chain kinase	only minor changes (in both directions)	22
Nucleic Acid Binding			
genesis (winged helix protein)	dsDNA	wing 2 motions quenched; wing 1 remains flexible	38
GCN4 (basic region Leu zipper protein)	dsDNA <sup>a</sup>	estimated reduction of entropy correlates with calorimetric data	39
topoisomerase I C-terminal domain	ssDNA	increased motions for most residues; decreased motion for a few	40
Wilms' tumor suppressor protein	dsDNA	reduced flexibility of zinc fingers that contact DNA; splice variant with KTS insertion exhibits reduced binding and increased flexibility of finger 4	41
Mrf-2 AT-rich interaction domain	dsDNA	predominant increases in flexibility; DNA-recognition elements display mixture of increases and decreases	<sup>c</sup>

<sup>a</sup> In these cases the holo form was not observed directly. <sup>b</sup> The apo form of stromelysin was not directly accessible to study. <sup>c</sup> Zhu et al. (unpublished results).

relaxation, although <sup>13</sup>C <sub>$\alpha$</sub>  relaxation data are also accessible. This approach has been applied to the binding of various proteins to metal ions,<sup>23–26</sup> small molecules,<sup>27–35</sup> peptides,<sup>22,36–37</sup> or nucleic acids.<sup>38–41</sup> The observed effects are summarized in Table 1.

Intuitively, one might anticipate that specific, high-affinity binding would require the formation of well-defined interactions (e.g., hydrogen bonds, salt bridges, van der Waals contacts, etc.) between a protein and its ligand. For such interactions to form, the conformation of the protein would need to be quite rigidly defined, whereas in the unbound form, the absence of these constraints may allow the protein a higher degree of flexibility. Thus, binding would be associated with loss of conformational entropy (i.e., "induced fit"), which would need to be more than offset by favorable enthalpic interactions (or increases in solvent entropy) for binding to be favored. In this light, entropy–enthalpy compensation is expected to be a common feature of many protein–ligand binding events, as discussed previously.<sup>42</sup>

Many of the NMR studies performed to date have revealed the anticipated loss in backbone entropy upon ligand binding (see Table 1). Furthermore, the observed rigidification of the structure is often localized at the ligand binding site.<sup>27,28,31,32,36,41</sup> Nevertheless, there have been a number of observations in which ligand binding has induced dynamic changes in regions distant from the binding site.<sup>23–25,32,33</sup> Perhaps even more surprisingly, there

are now several documented cases in which flexibility of certain regions increases upon binding.<sup>32–35,37,40</sup>

The observation of increased protein flexibility in response to ligand binding is important because it suggests that the conformational entropy of these residues actually promotes the process of ligand binding ( $\Delta G_{\text{conf}} = -T\Delta S_{\text{conf}}$  is negative, i.e., favorable). In several cases, distinct regions of the protein undergo compensating increases and decreases in entropy, so that the net effect is rather small.<sup>32–34,37</sup> For example, binding of an inhibitor to 4-oxalocrotonate tautomerase causes increased mobility of eight residues (notably, six are in the active site) and decreased mobility of seven residues, yielding a net estimate of  $\Delta G_{\text{conf}} \approx +5.4 \pm 4.6$  kJ/mol.<sup>34</sup> Similarly, binding of inhibitors to stromelysin or ribonuclease T1 quenches active site motions but increases the flexibility of regions distant from the active site.<sup>32,33</sup> In addition, three cases have been observed in which increases in backbone entropy upon binding far outweigh the observed decreases. These are discussed below.

Fesik and co-workers have described the dynamic changes of a topoisomerase domain upon binding to single-stranded DNA (ssDNA).<sup>40</sup> Binding induces a slight decrease in the flexibility of a few residues in loops and turns and a slight increase in the flexibility of many residues distributed throughout the secondary structure elements, some at the ssDNA binding surface. It was suggested that sliding of the DNA along the binding face

of the protein may occur in the complex and may be coupled to conformational rearrangements of the protein structure, in accord with the low specificity and low affinity of the interaction ( $K_d \approx 4 \mu\text{M}$ ).

Chen and colleagues (Zhu et al., unpublished results) have observed changes in the backbone flexibility of the AT-rich interaction domain Mrf-2 ARID upon specific binding to double-stranded DNA ( $K_d \approx 10\text{--}100 \text{ nM}$ ). One loop and the C-terminus both exhibit increases in NH order parameters on binding. Since these are part of the DNA-recognition surface, this observation supports an induced fit mechanism. On the other hand, another loop and a helix, both located at the binding surface, and several other structural elements undergo large decreases in  $S^2$ . The residues undergoing increased picosecond to nanosecond time scale motions far outnumber those with decreased motions, suggesting that backbone entropy may contribute significantly to the stability of the complex. Nevertheless, the observation of high flexibility in the binding interface of the complex (all recognition elements have average  $S^2 < 0.72$ ) raises the question of how binding specificity is maintained.

Recently, my co-workers and I have reported that binding of a small hydrophobic pheromone induces increased backbone flexibility throughout the structure of the mouse major urinary protein MUP-I.<sup>35</sup> The ligand binds into a central hydrophobic cavity in the protein such that it is completely occluded from solvent in the complex.<sup>43,44</sup> Assuming independence of NH group motions, the total change in backbone conformational free energy upon binding was estimated to be  $-52 \text{ kJ/mol}$  at  $30^\circ\text{C}$ , substantially more than the binding free energy ( $-34 \text{ kJ/mol}$ , corresponding to  $K_d \approx 1 \mu\text{M}$ ). Thus, even if the backbone entropy change is overestimated severalfold, it still appears to make a significant contribution to the overall stability of the complex. As suggested for topoisomerase I–ssDNA binding,<sup>40</sup> the enhanced protein flexibility in the complex is consistent with the low ligand specificity and modest affinity of MUP-I.

The increased flexibility of MUP-I upon pheromone binding has been rationalized in terms of the various physical effects anticipated to influence the affinity of small hydrophobic molecules for nonpolar cavities in proteins.<sup>35</sup> For small molecules ( $M_r < 300\text{--}400$ ), the magnitude of the classical hydrophobic effect (the favorable release of ordered water from hydrophobic surfaces) is not expected to outweigh the unfavorable loss of translational and rotational entropy sufficiently for micromolar affinity binding to occur.<sup>45</sup> Thus, binding requires additional favorable effects such as structural rearrangements, net formation of enthalpically favorable interactions, or increases in protein conformational entropy. Regarding the latter, we speculated that an ordered cluster of water molecules in the binding cavity may restrict the flexibility of the free MUP-I, whereas interactions between the pheromone and the walls of the cavity may be less specific, allowing an increase in protein motions.<sup>35</sup> This mechanism could potentially apply to other hydrophobic protein–ligand complexes. However,

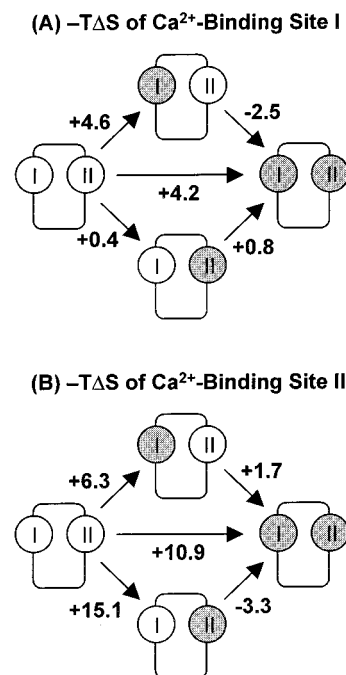


**FIGURE 4.** Schematic representation of the contributions of backbone entropy to the cooperativity of  $\text{Ca}^{2+}$  binding by calbindin  $\text{D}_{9k}$ . Values of  $-T\Delta S_{\text{conf}}$  (kJ/mol) estimated for residues in (A) the first and (B) the second  $\text{Ca}^{2+}$  binding sites are shown for each of the two possible binding pathways: binding site I filled first (top pathway of each figure) and binding site II filled first (bottom pathway of each figure). The filled binding sites are indicated by shading. This figure is derived from ref 24 (with permission).

this rationale predicts that binding should be entropy-driven, through a combination of increases in solvent entropy and protein conformational entropy, whereas new data now indicate that MUP-I–pheromone binding is an enthalpy-dominated process (unpublished results). A possible explanation for these results is that protein side chains may become rigidified, thus neutralizing the favorable increase in backbone entropy. Nevertheless, this type of analysis highlights the difficulty in comparing NMR-derived conformational entropy to the net change in entropy upon binding; the latter will often arise from small differences between large numbers.

## Backbone Entropy and Binding Cooperativity

The observation that ligand binding can sometimes induce changes in conformational flexibility in regions of the structure distant from the binding site raises the intriguing possibility that such dynamic changes could influence the cooperativity of ligand binding to multiple sites in the same protein. Chazin and co-workers have elegantly demonstrated that such a mechanism appears to be important in the cooperative binding of two calcium ions by the EF-hand protein calbindin  $\text{D}_{9k}$ .<sup>23,24</sup> Ion binding to either site (I or II) results in a slight decrease in site I flexibility and a dramatic decrease in site II flexibility. In contrast, binding the second ion gives rise to relatively small changes in order parameters. Figure 4 shows the estimated changes in conformational free energy of each binding site upon each binding step. Irrespective of the

binding pathway chosen, binding of the first ion results in a substantial net loss of conformational entropy for the two binding sites ( $\Delta G_{\text{conf}}$  estimated at +10.9 kJ/mol for site I binding and +15.5 kJ/mol for site II binding), whereas binding of the second ion induces a very slight net entropy increase ( $\Delta G_{\text{conf}}$  estimated at -0.8 kJ/mol for site II binding and -2.5 kJ/mol for site I binding). The reduction of entropy in the initial binding steps will tend to destabilize the intermediate states, hence making the second binding steps more favorable. Thus, the backbone entropy appears to make a contribution to the cooperative binding mechanism. The possibility that entropy modulation is involved more generally in site-site communication of EF-hand proteins is supported by the observation<sup>25</sup> that binding of calcium to site II of cardiac troponin C decreases the backbone conformational free energy of both binding sites (by an estimated 2.1 and 9.2 kJ/mol for sites I and II, respectively), even though site I is not capable of calcium binding.

### Side Chain Entropy and Ligand Binding

The studies of backbone flexibility discussed above have been complemented by several studies of changes in side chain dynamics induced by ligands. Dynamics data are derived from <sup>13</sup>C or <sup>2</sup>H relaxation properties of appropriately labeled side chain methyl groups and are reported as  $S^2_{\text{axis}}$  values, representing the degree of motional restriction of methyl group symmetry axes.<sup>46</sup>

The dynamics of 11 leucine side chains have been compared for Staphylococcal nuclease in its apo form and bound to both Ca<sup>2+</sup> and thymidine 3',5'-bisphosphate (pdTp).<sup>47</sup> Six residues, all located within 10 Å of the ligands, exhibit significant increases in  $S^2_{\text{axis}}$  upon binding, with the largest changes observed for residues closest to the active site; none of the leucine residues located more than 10 Å from the ligands exhibits a significant change in  $S^2_{\text{axis}}$ . The data support a local rigidification of the structure in the vicinity of the ligands, suggesting that loss of conformational entropy is compensated by formation of enthalpically favorable interactions.

Kay, Forman-Kay, and co-workers have characterized the dynamics of two SH2 domains both free and in complexes with their cognate phosphotyrosine-containing peptides.<sup>37,48,49</sup> The average backbone NH order parameter of the C-terminal SH2 domain of phospholipase C- $\gamma$ 1 does not change significantly upon binding of a peptide.<sup>37</sup> However, one residue that interacts with the phosphotyrosine moiety is dramatically rigidified, and several residues interacting with the hydrophobic region of the peptide become more flexible upon binding. Side chain methyl groups display a similar distribution of dynamics, with the phosphotyrosine binding site undergoing a disorder-to-order transition upon binding while the hydrophobic binding site retains significant flexibility.<sup>48</sup> The selective rigidification of the phosphotyrosine binding site can be rationalized by noting that interactions in this site make the primary contribution to the SH2-peptide binding energy, whereas residues in the hydrophobic site contrib-

ute little (<4 kJ/mol) to the interaction energy.<sup>49</sup> Apparently, loss of entropy in the phosphotyrosine binding site is offset by significant (presumably enthalpic) contributions to binding. This idea of enthalpy-entropy compensation is further supported by studies of the N-terminal SH2 domain of Syp tyrosine phosphatase and its cognate peptide.<sup>49</sup> In this case, the binding energy is distributed differently, with the contribution of hydrophobic residues exceeding 12 kJ/mol. Correspondingly, a significant loss of side chain motion upon binding occurs for residues interacting with either the phosphotyrosine residue or the hydrophobic residues of the peptide.

Further support for enthalpy-entropy compensation upon peptide binding is provided by Wand and co-workers' study of the binding between calmodulin and a peptide derived from myosin light chain kinase.<sup>22</sup> In this case, binding causes only very minor changes in backbone NH group dynamics, but many of the methyl-containing side chains undergo dramatic changes in  $S^2_{\text{axis}}$  values. Two active site methionine side chains and several other residues that make hydrophobic contacts with the peptide become significantly more rigid upon binding, suggesting that specific enthalpic interactions are sufficient to overcome the loss of entropy for these side chains. In addition, several other residues more distant from the binding interface also experience losses in side chain entropy, and a few surface-exposed side chains gain mobility upon binding. Changes in side chain entropy upon binding are estimated to cost as much as 146 kJ/mol; the total binding free energy is -50 kJ/mol. Again, if the conformational entropy estimate is correct to within even an order of magnitude, then modulation of side chain entropy needs to be recognized as an important factor influencing binding affinity. Furthermore, the observation of changes in side chain mobility without corresponding changes in the backbone suggests a low level of correlation between the motions of these structural elements.

Finally, a possible role for protein side chain entropy in controlling enzyme catalysis is suggested by a study of a tyrosine residue in the active site of  $\Delta^5$ -3-ketosteroid isomerase, both free and in the presence of a steroidal analogue of the reaction product.<sup>50</sup> The phenolic side chain of Tyr-14 is proposed to act as a general acid, forming a strong hydrogen bond to the keto group of the substrate and an even stronger hydrogen bond to the dienolic intermediate, thus stabilizing the intermediate. Binding of the product analogue significantly decreases the high-frequency motion of the Tyr-14 side chain but does not affect backbone flexibility; the loss in side chain flexibility was previously suggested on the basis of UV-absorption bandwidths.<sup>51</sup> The observed loss of side chain entropy is expected to be compensated by the newly formed Tyr-14-ligand hydrogen bond. In addition, loss of side chain entropy during the initial binding step may facilitate formation of the reaction transition state by reducing the entropy barrier for the catalytic step.<sup>50</sup> It is possible that this effect also operates in the catalytic mechanisms of other enzymes.

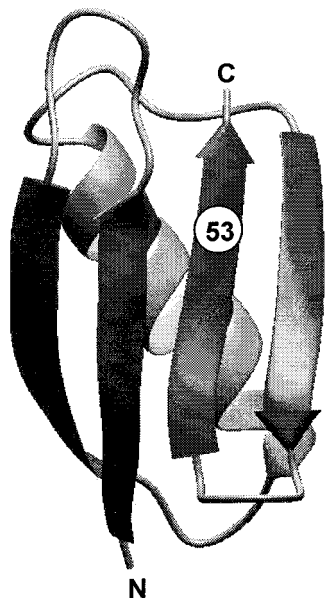


**FIGURE 5.** B1 domain of Streptococcal protein G, showing the position of residue 53 on the outer surface of the  $\beta$ -sheet. Mutation of this residue (from wild-type Thr to Ala or Met) causes correlated changes in backbone entropy and protein stability without significantly disrupting the average native structure of the domain.<sup>56</sup> The mutations are made in the context of neighboring amino acids introduced to minimize cross-strand interactions. Thus, their relative stabilities are related to the intrinsic  $\beta$ -sheet propensities of the amino acid at position 53.<sup>55</sup>

### Backbone Entropy and Protein Stability

Proteins are expected to undergo dramatic losses in conformational entropy upon folding,<sup>6</sup> as illustrated by the protein folding funnel (Figure 1) and supported by (among other things) NMR relaxation data interpreted using the reduced spectral density approach.<sup>52–54</sup> In theory, it would be possible to use methods similar to those described above to estimate the difference in conformational entropy between unfolded and folded forms of a protein. However, this is difficult in practice because (1) separation of the effects of global tumbling and internal motions is no longer meaningful for unfolded proteins that lack stable global folds; (2) there may be substantial differences in the predominant time scales (as well as amplitudes) of internal motions upon denaturation; and (3) the nature and extent of correlated motions may undergo dramatic changes on unfolding.

To circumvent these problems, we have begun to address the relationship between conformational entropy and protein stability by comparing the dynamics of three  $\beta$ -sheet mutants<sup>55</sup> of the B1 domain of Streptococcal protein G in their folded states (Figure 5).<sup>56</sup> Since the structures of these mutants are essentially identical, and the degree of motional correlation can be assumed to be similar for all three (to a first approximation), differences between the NMR-derived order parameters are likely to provide a reasonable indication of the true differences in the conformational entropy of the folded states. If the additional assumption is made that the conformational entropy of the unfolded state is similar for all three

**Table 2. Thermodynamic Parameters for B1 Domain Mutants**

	Met-53	Thr-53
$\Delta G_{\text{conf}}$ (kJ/mol) <sup>a,b</sup>	–4.3	–14.2
$\Delta\Delta G_{\text{folding}}$ (kJ/mol) <sup>a,c</sup>	–4.2	–8.9
$\Delta\Delta A_{\text{folding}}$ (kJ/mol) <sup>a,d</sup>	–2.5	–6.3

<sup>a</sup> All changes are relative to the Ala-53 mutant. <sup>b</sup> Estimated from NH order parameters.<sup>56</sup> <sup>c</sup> Determined from denaturation experiments.<sup>55</sup> <sup>d</sup> Calculated from steric considerations.<sup>57</sup>

mutants, then the differences estimated from comparisons of the folded states should reflect the contributions of conformational entropy to the relative folding free energies of the mutants.

As shown in Table 2, the estimated conformational free energy ( $G_{\text{conf}}$ ) of the B1 domain mutants varies in the same direction and with magnitude similar to that of the overall folding stability ( $\Delta G_{\text{folding}}$ ),<sup>55</sup> suggesting that backbone entropy makes a contribution to differences in folding stability.<sup>56</sup> This possibility had been suggested previously by the calculations of Street and Mayo ( $\Delta\Delta A$  values in Table 2).<sup>57</sup> However, the latter calculations take into account only local variations in conformational freedom, whereas the differences in conformational entropy between the B1 domain mutants are distributed throughout the domain. The latter observation suggests that backbone motions in the B1 domain may be highly cooperative, supporting the likely existence of correlated motions.

The proposal that increased backbone flexibility can stabilize a protein structure is at first counterintuitive because one might anticipate that an increase in motion would be accompanied by a loss of enthalpic interactions (such as secondary structure hydrogen bonds), leading to denaturation of the protein. However, the differences in average order parameters observed for the B1 domain mutants (Table 1) correspond to only a  $\sim 2^\circ$  variation in cone semiangle, when interpreted according to the diffusion-in-a-cone model. Such a small increase in motional amplitude could clearly be accommodated without global disruption of the structure. In fact, the variation of order parameters within the secondary structure regions of the most rigid mutant corresponds to cone semiangles in a much wider range ( $\sim 22$ – $30^\circ$ ). Similarly, variable-temperature studies of the wild-type B1 domain<sup>58</sup> indicate that an increase in average cone semiangle from  $24^\circ$  (at  $20^\circ\text{C}$ ) to  $33^\circ$  (at  $50^\circ\text{C}$ ) can be readily accommodated without loss of global structure (the protein denatures at  $89^\circ\text{C}$ ).

### Conformational Heat Capacity and Protein Stability

The methods described above for estimation of conformational entropy can be extended to allow estimation of the heat capacity associated with bond vector fluctuations from the temperature dependence of  $S_{\text{conf}}$ .<sup>17,59</sup>

$$C_{\text{p,conf}} = \frac{dS_{\text{conf}}}{d \ln(T)} \quad (2)$$

Obviously, the validity of  $C_{\text{p,conf}}$  values derived in this way

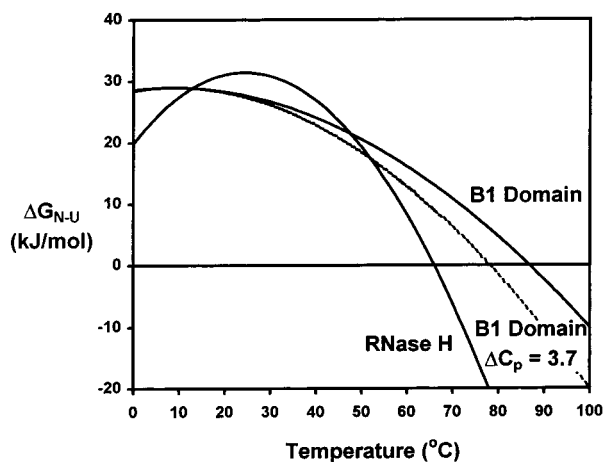


**FIGURE 6.** Comparison of the experimentally determined thermal stability profiles (solid curves) for the wild-type B1 domain of Streptococcal protein G<sup>61</sup> and RNase H.<sup>62</sup> The experimental  $\Delta C_{p,N-U}$  values are 2.9 and 11.3 kJ/mol·K for RNase H and the B1 domain, respectively. The dotted curve is the simulated stability profile of the B1 domain with  $\Delta C_{p,N-U}$  increased from 2.9 to 3.7 kJ/mol·K, but the enthalpy and entropy changes at 9 °C (the temperature of maximum stability) the same as the experimental values. These curves were generated according to eq 3. Reprinted from ref 58 with permission. Copyright 2000.

is also subject to the limitations discussed above for the entropy estimation.

The role of heat capacity in controlling protein stability is represented by the equation<sup>6,60</sup>

$$\Delta G_{N-U} = \Delta H_0 - T\Delta S_0 + \Delta C_{p,N-U}[T - T_0 - T \ln(T/T_0)] \quad (3)$$

in which  $\Delta G_{N-U}$  is the free energy of denaturation,  $\Delta H_0$  and  $\Delta S_0$  are the corresponding enthalpy and entropy changes, respectively, at a reference temperature,  $T_0$ , and  $\Delta C_{p,N-U}$  is the change in heat capacity at constant pressure, which is assumed to be invariant with temperature. The curvature of the thermal stability profile is determined by the value of  $\Delta C_{p,N-U}$ , as illustrated in Figure 6 for the wild-type B1 domains of protein G<sup>61</sup> and ribonuclease H.<sup>62</sup> Thus, small variations in heat capacity can profoundly influence the stability of a protein at extreme temperatures.

Gomez et al.<sup>63</sup> have estimated that the heat capacity of a folded protein is typically partitioned into contributions from fluctuations of the primary (covalent) structure (~82%), of noncovalent interactions within the protein molecule (~3%), and of protein–solvent or solvent–solvent interactions (~15%). The heat capacity of unfolding is influenced most strongly by changes in the latter term because denaturation involves substantial solvation of the protein; typically,  $\Delta C_{p,N-U}$  is roughly proportional to the hydrophobic surface area exposed upon denaturation.<sup>61,64</sup> Nevertheless, it remains possible that subtle changes in the first two contributions to heat capacity (referred to collectively here as “conformational heat capacity”,  $C_{p,conf}$ ) have some influence on the thermal stability profile.

Derivation of heat capacity from the temperature dependence of order parameters provides the component of  $C_{p,conf}$  resulting from the internal rotational motions of individual bond vectors on the observable time scale. This approach has now been applied to several folded or unfolded proteins;<sup>17,58,59,65</sup> typical  $C_{p,conf}$  values obtained are on the order of ~10–50 J/mol·K per residue. Of particular interest,  $C_{p,conf}$  values in the secondary structure regions of the wild-type B1 domain<sup>58</sup> are significantly higher than those reported for secondary structure regions of a mutant calmodulin domain.<sup>59</sup> The difference corresponds to a lower heat capacity of denaturation ( $\Delta C_{p,N-U}$ ) for the B1 domain by as much as ~0.8 kJ/mol·K; i.e., if the  $C_{p,conf}$  values of the B1 domain were similar to those in the calmodulin domain,  $\Delta C_{p,N-U}$  could be ~0.8 kJ/mol·K higher (3.7 rather than 2.9 kJ/mol·K), causing the melting temperature of the B1 domain to be ~9 °C lower (see Figure 6).<sup>58</sup> Despite the low precision of  $C_{p,conf}$  estimates derived from order parameters and the difficulties associated with the assumption of independent bond vector fluctuations, the current data suggest that changes in conformational heat capacity could have a measurable effect on protein stability at extreme temperatures. A similar suggestion has recently been put forward on the basis of neutron scattering data for mesophilic and thermophilic  $\alpha$ -amylases.<sup>66</sup>

## Summary and Future Directions

The studies discussed above provide convincing evidence that variations in the entropy associated with picosecond to nanosecond time scale motions can, in some cases, have a significant influence on the stabilities of protein–ligand complexes or the relative stabilities of protein mutants. Backbone and side chain flexibility can either decrease or increase upon ligand binding. Decreases are often associated with “enthalpy–entropy compensation” and “induced fit” binding, whereas increases in conformational entropy can contribute to stabilization of complexes. In certain cases, conformational entropy appears to play a role in cooperative binding and enzyme catalysis. Furthermore, there are now indications that variations in conformational entropy and heat capacity may both be important in stabilizing the folded structures of proteins.

Despite the exciting progress in this field over the past several years, some important issues remain to be resolved. First, as discussed above, the accuracy of entropy estimates obtained from order parameters remains seriously compromised by the limited number of bond vectors and limited time scale of motions that are observable, the insensitivity of relaxation parameters to translational motion, and the requirement to assume independence of bond vector motions. Second, although changes in dynamics are observable, the mechanisms that underlie these changes are poorly understood, and the results are often difficult to rationalize. In the case of induced fit, restriction of motion is presumably coupled to formation of enthalpically favorable interactions. However, in cases for which increases of conformational fluctuations are



observed or when regions distant from the binding site undergo changes in dynamics, the mechanisms are much less obvious and may involve changes in solvation, subtle packing interactions, hydrogen bond strengths, networks of interactions, etc. Experimental approaches to understanding these mechanisms will likely require the painstaking analysis of families of mutants (or complexes with ligand analogues) with subtle differences in structure and dynamics.

An attractive approach to understanding the role of entropy variation in binding and stability is to combine experimental dynamics measurements with theoretical approaches such as molecular dynamics (MD) and normal-mode analysis. Several comparisons have been made between order parameters derived from NMR and MD.<sup>67–69</sup> In general, MD simulations tend to correctly identify the most flexible structural regions, but subtle variations in NMR-derived order parameters are not well reproduced, presumably due to deficiencies in one or both method(s). Extension of MD simulation times to several nanoseconds or longer may improve the agreement with experiment. It may be possible in the future to use experimental relaxation data to fine-tune MD force fields, affording better prediction of experimental results. If good agreement could be achieved between experimental and calculated data, the latter could be used to assess the nature of internal motions, the nature and extent of correlated motions, and internal conformational entropy. The recent computational approach of Brüschweiler and co-workers,<sup>70,71</sup> in which NMR-detectable reorientational motions are separated from other intramolecular motions, may be an important breakthrough in the comparison of experimental and computational dynamics data; this approach has already been used to assess the influence of motional correlations on entropy changes. Ultimately, such improved computational methods may even allow conformational entropy to be taken into account in the prediction of binding affinities and drug design.

*I am indebted to Drs. Walter J. Chazin and Mikael Akke for their critical reading of the manuscript and to the reviewers for helpful comments. I also thank Drs. Yuan Chen and Peter E. Wright for providing copies of unpublished manuscripts. Work on protein dynamics in my laboratory has been supported by the National Science Foundation (MCB-9600968), the National Institutes of Health (GM-55055), the American Chemical Society Petroleum Research Fund, and the American Heart Association National Affiliate (Established Investigator Award).*

## References

- Palmer, A. G.; Williams, J.; McDermott, A. Nuclear Magnetic Resonance Studies of Biopolymer Dynamics. *J. Phys. Chem.* **1996**, *100*, 13293–13310.
- Fischer, M. W. F.; Majumdar, A.; Zuiderweg, E. R. P. Protein NMR Relaxation: Theory, Applications and Outlook. *Prog. Nucl. Magn. Reson. Spectrosc.* **1998**, *33*, 207–272.
- Kay, L. E. Protein Dynamics From NMR. *Nat. Struct. Biol.* **1998**, *Suppl. 5*, 513–517.
- Ishima, R.; Torchia, D. A. Protein Dynamics From NMR. *Nat. Struct. Biol.* **2000**, *7*, 740–743.
- Brooks, C. L., III; Gruebele, M.; Onuchic, J. N.; Wolynes, P. G. Chemical Physics of Protein Folding. *Proc. Natl. Acad. Sci. U.S.A.* **1998**, *95*, 11037–11038.
- Creighton, T. E. *Proteins: Structures and Molecular Properties*; W. H. Freeman and Co.: New York, 1993; pp 18–19.
- Abragam, A. *Principles of Nuclear Magnetism*; Clarendon Press: Oxford, 1961; pp 1–599.
- Peng, J. W.; Wagner, G. Mapping of the Spectral Densities of N–H Bond Motions in Eglin c Using Heteronuclear Relaxation Experiments. *Biochemistry* **1992**, *31*, 8571–8586.
- Lipari, G.; Szabo, A. Model-Free Approach to the Interpretation of Nuclear Magnetic Resonance Relaxation in Macromolecules. 1. Theory and Range of Validity. *J. Am. Chem. Soc.* **1982**, *104*, 4546–4559.
- Lipari, G.; Szabo, A. Model-Free Approach to the Interpretation of Nuclear Magnetic Resonance Relaxation in Macromolecules. 2. Analysis of Experimental Results. *J. Am. Chem. Soc.* **1982**, *104*, 4559–4570.
- Clare, G. M.; Driscoll, P. C.; Wingfield, P. T.; Gronenborn, A. M. Analysis of the Backbone Dynamics of Interleukin-1 $\beta$  Using Two-Dimensional Inverse Detected Heteronuclear <sup>15</sup>N–<sup>1</sup>H NMR Spectroscopy. *Biochemistry* **1990**, *29*, 7387–7401.
- Clare, G. M.; Szabo, A.; Bax, A.; Kay, L. E.; Driscoll, P. C.; Gronenborn, A. M. Deviations From the Simple Two-Parameter Model-Free Approach to the Interpretation of Nitrogen-15 Nuclear Magnetic Relaxation of Proteins. *J. Am. Chem. Soc.* **1990**, *112*, 4989–4991.
- Kay, L. E.; Torchia, D. A.; Bax, A. Backbone Dynamics of Proteins As Studied by <sup>15</sup>N Inverse Detected Heteronuclear NMR Spectroscopy: Application to Staphylococcal Nuclease. *Biochemistry* **1989**, *28*, 8972–8979.
- Akke, M.; Brüschweiler, R.; Palmer, A. G., III. NMR Order Parameters and Free Energy: an Analytical Approach and Its Application to Cooperative Ca<sup>2+</sup> Binding by Calbindin D<sub>9k</sub>. *J. Am. Chem. Soc.* **1993**, *115*, 9832–9833.
- Li, Z.; Raychaudhuri, S.; Wand, A. J. Insights into the Local Residual Entropy of Proteins Provided by NMR Relaxation. *Protein Sci.* **1996**, *5*, 2647–2650.
- Yang, D. W.; Kay, L. E. Contributions to Conformational Entropy Arising From Bond Vector Fluctuations Measured From NMR-Derived Order Parameters: Application to Protein Folding. *J. Mol. Biol.* **1996**, *263*, 369–382.
- Yang, D.; Yu-Keung, M.; Forman-Kay, J. D.; Farrow, N. A.; Kay, L. E. Contributions to Protein Entropy and Heat Capacity From Bond Vector Motions Measured by NMR Spin Relaxation. *J. Mol. Biol.* **1997**, *272*, 790–804.
- Daragan, V. A.; Mayo, K. H. Analysis of Internally Restricted Correlated Rotations in Peptides and Proteins Using C-13 and N-15 NMR Relaxation Data. *J. Phys. Chem.* **1996**, *100*, 8378–8388.
- Lemaster, D. M.; Kushlan, D. M. Dynamical Mapping of E. Coli Thioredoxin Via C-13 NMR Relaxation Analysis. *J. Am. Chem. Soc.* **1996**, *118*, 9255–9264.
- Lemaster, D. M. NMR relaxation order parameter analysis of the dynamics of protein side chains. *J. Am. Chem. Soc.* **1999**, *121*, 1726–1742.
- Goodman, J. L.; Pagel, M. D.; Stone, M. J. Relationships Between Protein Structure and Dynamics From a Database of NMR-Derived Backbone Order Parameters. *J. Mol. Biol.* **2000**, *295*, 963–978.
- Lee, A. L.; Kinnear, S. A.; Wand, A. J. Redistribution and Loss of Side Chain Entropy Upon Formation of a Calmodulin–Peptide Complex. *Nat. Struct. Biol.* **2000**, *7*, 72–77.
- Akke, M.; Skelton, N. J.; Kördel, J.; Palmer, A. G., III; Chazin, W. J. Effects of Ion Binding on the Backbone Dynamics of Calbindin D<sub>9k</sub> Determined by <sup>15</sup>N NMR Relaxation. *Biochemistry* **1993**, *32*, 9832–9844.
- Maler, L.; Blankenship, J.; Rance, M.; Chazin, W. J. Site–Site Communication in the EF-Hand Ca<sup>2+</sup>-Binding Protein Calbindin D<sub>9k</sub>. *Nat. Struct. Biol.* **2000**, *7*, 245–250.
- Spyropoulos, L.; Gagne, S. M.; Li, M. X.; Sykes, B. D. Dynamics and Thermodynamics of the Regulatory Domain of Human Cardiac Troponin C in the Apo- and Calcium-Saturated States. *Biochemistry* **1998**, *37*, 18032–18044.
- Gagne, S. M.; Tsuda, S.; Spyropoulos, L.; Kay, L. E.; Sykes, B. D. Backbone and Methyl Dynamics of the Regulatory Domain of Troponin C: Anisotropic Rotational Diffusion and Contribution of Conformational Entropy to Calcium Affinity. *J. Mol. Biol.* **1998**, *278*, 667–686.
- Cheng, J. W.; Lepre, C. A.; Moore, J. M. <sup>15</sup>N NMR Relaxation Studies of the FK506 Binding Protein: Dynamic Effects of Ligand Binding and Implications for Calcineurin Recognition. *Biochemistry* **1994**, *33*, 4093–4100.
- Rischel, C.; Madsen, J. C.; Andersen, K. V.; Poulsen, F. M. Comparison of Backbone Dynamics of Apo- and Holo-Acyl-Coenzyme A Binding Protein Using <sup>15</sup>N Relaxation Measurements. *Biochemistry* **1994**, *33*, 13997–14002.
- Hodsdon, M. E.; Cistola, D. P. Discrete Backbone Disorder in the Nuclear Magnetic Resonance Structure of Apo Intestinal Fatty Acid-Binding Protein: Implications for the Mechanism of Ligand Entry. *Biochemistry* **1997**, *36*, 1450–1460.

- (30) Hodsdon, M. E.; Cistola, D. P. Ligand Binding Alters the Backbone Mobility of Intestinal Fatty Acid-Binding Protein As Monitored by N-15 NMR Relaxation and H-1 Exchange. *Biochemistry* **1997**, *36*, 2278–2290.
- (31) Scrofani, S. D. B.; Chung, J.; Huntley, J. J. A.; Benkovic, S. J.; Wright, P. E.; Dyson, H. J. NMR Characterization of the Metallo- $\beta$ -lactamase from *Bacteroides fragilis* and Its Interaction with a Tight-Binding Inhibitor: Role of an Active-Site Loop. *Biochemistry* **1999**, *38*, 14507–14514.
- (32) Fushman, D.; Weisemann, R.; Thuring, H.; Rüterjans, H. Backbone Dynamics of Ribonuclease T1 and Its Complex With 2'GMP Studied by Two-Dimensional Heteronuclear NMR Spectroscopy. *J. Biomol. NMR* **1994**, *4*, 61–78.
- (33) Yuan, P.; Marshall, V. P.; Petzold, G. L.; Poorman, R. A.; Stockman, B. J. Dynamics of Stromelysin/Inhibitor Interactions Studied by <sup>15</sup>N NMR Relaxation Measurements: Comparison of Ligand Binding to the S1–S3 and S'1–S'3 Subsites. *J. Biomol. NMR* **1999**, *15*, 55–64.
- (34) Stivers, J. T.; Abeygunawardana, C.; Mildvan, A. S. <sup>15</sup>N NMR Relaxation Studies of Free and Inhibitor-Bound 4-Oxalocrotonate Tautomerase: Backbone Dynamics and Entropy Changes of an Enzyme Upon Inhibitor Binding. *Biochemistry* **1996**, *35*, 16036–16047.
- (35) Zidek, L.; Novotny, M. V.; Stone, M. J. Increased Protein Backbone Conformational Entropy Upon Hydrophobic Ligand Binding. *Nat. Struct. Biol.* **1999**, *6*, 1118–1121.
- (36) Olejniczak, E. T.; Zhou, M. M.; Fesik, S. W. Changes in the NMR-Derived Motional Parameters of the Insulin Receptor Substrate 1 Phosphotyrosine Binding Domain Upon Binding to an Interleukin 4 Receptor Phosphopeptide. *Biochemistry* **1997**, *36*, 4118–4124.
- (37) Farrow, N. A.; Muhandiram, R.; Singer, A. U.; Pascal, S. M.; Kay, C. M.; Gish, G.; Shoelson, S. E.; Pawson, T.; Forman-Kay, J. D.; Kay, L. E. Backbone Dynamics of a Free and a Phosphopeptide-Complexed Src Homology 2 Domain Studied by <sup>15</sup>N NMR Relaxation. *Biochemistry* **1994**, *33*, 5984–6003.
- (38) Jin, C.; Liao, X. Backbone Dynamics of a Winged Helix Protein and Its DNA Complex at Different Temperatures: Changes of Internal Motions in Genesis Upon Binding to DNA. *J. Mol. Biol.* **1999**, *292*, 641–651.
- (39) Bracken, C.; Carr, P. A.; Cavanagh, J.; Palmer, A. G., III. Temperature Dependence of Intramolecular Dynamics of the Basic Leucine Zipper of GCN4: Implications for the Entropy of Association With DNA. *J. Mol. Biol.* **1999**, *285*, 2133–2146.
- (40) Yu, L.; Zhu, C. X.; Tse-Dinh, Y. C.; Fesik, S. W. Backbone Dynamics of the C-Terminal Domain of *Escherichia coli* Topoisomerase I in the Absence and Presence of Single-Stranded DNA. *Biochemistry* **1996**, *35*, 9661–9666.
- (41) Laity, J. L.; Dyson, H. J.; Wright, P. E. Molecular Basis for Modulation of Biological Function by Alternate Splicing of the Wilms' Tumor Suppressor Protein. *Proc. Natl. Acad. Sci. U.S.A.* **2000**, in press.
- (42) Dunitz, J. D. Win Some, Lose Some: Enthalpy–Entropy Compensation in Weak Intermolecular Interactions. *Chem Biol.* **1995**, *2*, 709–712.
- (43) Zidek, L.; Stone, M. J.; Lato, S. M.; Pagel, M. D.; Miao, Z.; Ellington, A. D.; Novotny, M. V. NMR Mapping of the Recombinant Mouse Major Urinary Protein I Binding Site Occupied by the Pheromone 2-sec-Butyl-4,5-dihydrothiazole. *Biochemistry* **1999**, *38*, 9850–9861.
- (44) Bocskai, Z.; Groom, C. R.; Flower, D. R.; Wright, C. E.; Phillips, S. E. V.; Cavaggioni, A.; Findlay, J. B. C.; North, A. C. T. Pheromone binding to two rodent urinary proteins revealed by X-ray crystallography. *Nature* **1992**, *360*, 186–188.
- (45) Janin, J.; Chothia, C. Role of Hydrophobicity in the Binding of Coenzymes. *Biochemistry* **1978**, *17*, 2943–2948.
- (46) Lee, A. L.; Flynn, P. F.; Wand, A. J. Comparison of <sup>2</sup>H and <sup>13</sup>C NMR Relaxation Techniques for the Study of Protein Methyl Group Dynamics in Solution. *J. Am. Chem. Soc.* **1999**, *121*, 2891–2902.
- (47) Nicholson, L. K.; Kay, L. E.; Baldisseri, D. M.; Arango, J.; Young, P. E.; Bax, A.; Torchia, D. A. Dynamics of Methyl Groups in Proteins As Studied by Proton-Detected <sup>13</sup>C NMR Spectroscopy. Application to the Leucine Residues of Staphylococcal Nuclease. *Biochemistry* **1992**, *31*, 5253–5263.
- (48) Kay, L. E.; Muhandiram, D. R.; Farrow, N. A.; Aubin, Y.; Forman-Kay, J. D. Correlation between Dynamics and High Affinity Binding in an SH2 Domain Interaction. *Biochemistry* **1996**, *35*, 361–368.
- (49) Kay, L. E.; Muhandiram, D. R.; Wolf, G.; Shoelson, S. E.; Forman-Kay, J. D. Correlation Between Binding and Dynamics at SH2 Domain Interfaces. *Nat. Struct. Biol.* **1998**, *5*, 156–163.
- (50) Zhao, Q.; Abeygunawardana, C.; Mildvan, A. S. <sup>13</sup>C NMR Relaxation Studies of Backbone and Side Chain Motion of the Catalytic Tyrosine Residue in Free and Steroid-Bound  $\Delta^5$ -3-Ketosteroid Isomerase. *Biochemistry* **1996**, *35*, 1525–1532.
- (51) Zhao, Q.; Li, Y. K.; Mildvan, A. S.; Talalay, P. Ultraviolet Spectroscopic Evidence for Decreased Motion of the Active Site Tyrosine Residue of  $\Delta^5$ -3-Ketosteroid Isomerase by Steroid Binding. *Biochemistry* **1995**, *34*, 6562–6572.
- (52) Farrow, N. A.; Zhang, O. W.; Formankay, J. D.; Kay, L. E. Characterization of the Backbone Dynamics of Folded and Denatured States of an SH3 Domain. *Biochemistry* **1997**, *36*, 2390–2402.
- (53) Eliezer, D.; Chung, J.; Dyson, H. J.; Wright, P. E. Native and Non-Native Secondary Structure and Dynamics in the PH 4 Intermediate of Apomyoglobin. *Biochemistry* **2000**, *39*, 2894–2901.
- (54) Eliezer, D.; Yao, J.; Dyson, H. J.; Wright, P. E. Structural and Dynamic Characterization of Partially Folded States of Apomyoglobin and Implications for Protein Folding. *Nat. Struct. Biol.* **1998**, *5*, 148–155.
- (55) Smith, C. K.; Withka, J. M.; Regan, L. A Thermodynamic Scale for the  $\beta$ -Sheet Forming Tendencies of the Amino Acids. *Biochemistry* **1994**, *33*, 5510–5517.
- (56) Stone, M. J.; Gupta, S.; Snyder, N.; and Regan, L. Comparison of Protein Backbone Entropy and  $\beta$ -Sheet Stability: NMR-Derived Dynamics of Protein G B1 Domain Mutants. *J. Am. Chem. Soc.* **2001**, *123*, 185–186.
- (57) Street, A. G.; Mayo, S. L. Intrinsic  $\beta$ -Sheet Propensities Result From van der Waals Interactions Between Side Chains and the Local Backbone. *Proc. Natl. Acad. Sci. U.S.A.* **1999**, *96*, 9074–9076.
- (58) Seewald, M. J.; Pichumani, K.; Stowell, C.; Tibbals, B. V.; Regan, L.; Stone, M. J. The Role of Backbone Conformational Heat Capacity in Protein Stability: Temperature-Dependent Dynamics of the B1 Domain of Streptococcal Protein G. *Protein Sci.* **2000**, *9*, 1177–1193.
- (59) Evenas, J.; Forsen, S.; Malmendal, A.; Akke, M. Backbone Dynamics and Energetics of a Calmodulin Domain Mutant Exchanging Between Closed and Open Conformations. *J. Mol. Biol.* **1999**, *289*, 603–617.
- (60) Fersht, A. *Structure and Mechanism in Protein Science*; W. H. Freeman and Co.: New York, 1999.
- (61) Alexander, P.; Fahnestock, S.; Lee, T.; Orban, J.; Bryan, P. Thermodynamic Analysis of the Folding of the Streptococcal Protein G IgG-Binding Domains B1 and B2: Why Small Proteins Tend To Have High Denaturation Temperatures. *Biochemistry* **1992**, *31*, 3597–3603.
- (62) Hollien, J.; Marqusee, S. A Thermodynamic Comparison of Mesophilic and Thermophilic Ribonucleases H. *Biochemistry* **1999**, *38*, 3831–3836.
- (63) Gomez, J.; Hilsner, V.; Xie, D.; Freire, E. The Heat Capacity of Proteins. *Proteins: Struct., Funct., Genet.* **1995**, *22*, 404–412.
- (64) Privalov, P. L.; Gill, S. J. Stability of Protein Structure and Hydrophobic Interaction. *Adv. Protein Chem.* **1988**, *39*, 191–234.
- (65) Mandel, A. M.; Akke, M.; Palmer, A. G. Dynamics of Ribonuclease H: Temperature Dependence of Motions on Multiple Time Scales. *Biochemistry* **1996**, *35*, 16009–16023.
- (66) Fitter, J.; Heberle, J. Structural Equilibrium Fluctuations in Mesophilic and Thermophilic  $\alpha$ -Amylases. *Biophys. J.* **2000**, *79*, 1629–1636.
- (67) Smith, L. J.; Mark, A. E.; Dobson, C.; van Gunsteren, W. F. Comparison of MD Simulations and NMR Experiments for Hen Lysozyme. Analysis of Local Fluctuations, Cooperative Motions, and Global Changes. *Biochemistry* **1995**, *34*, 10918–10931.
- (68) Philippopoulos, M.; Lim, C. Molecular Dynamics Simulation of E. Coli Ribonuclease H-1 in Solution: Correlation With NMR and X-Ray Data and Insights into Biological Function. *J. Mol. Biol.* **1995**, *254*, 771–792.
- (69) Philippopoulos, M.; Mandel, A. M.; Palmer, A. G., III; Lim, C. Accuracy and Precision of NMR Relaxation Experiments and MD Simulations for Characterizing Protein Dynamics. *Proteins* **1997**, *28*, 481–493.
- (70) Prompers, J. J.; Brunschweiler, R. Thermodynamic Interpretation of NMR Relaxation Parameters in Proteins in the Presence of Motional Correlations. *J. Phys. Chem. B* **2000**, *104*, 11416–11424.
- (71) Prompers, J. J.; Scheurer, C.; Brunschweiler, R. Characterization of NMR Relaxation-active Motions of a Partially Folded A-state Analogue of Ubiquitin. *J. Mol. Biol.* **2001**, *305*, 1085–1097.

AR000079C